Available online at www.sciencedirect.com

SciVerse ScienceDirect

Physics Procedia 25 (2012) 86 – 91

Physics Procedia

2012 International Conference on Solid State Devices and Materials Science

Effect of Field Plate on the RF Performance of AlGaN/GaN HEMT Devices

Che-Yang Chiang[a], Heng-Tung Hsu[a*], and Edward Yi Chang[b]

[a*]*Department of Communications Engineering, Yuan Ze University, ChungLi, Taiwan, 32003*
[b]*Department of Material Science, National Chiao Tung University, Hsinchu, Taiwan, 30010*

Abstract

This paper examines the effect of the field plate structure on the RF performance of AlGaN/GaN High Electron Mobility Transistor (HEMT) devices. While the field plate structure helps to increase the breakdown voltage of the device through modulating the electric field locally, it induces additional feedback capacitance from drain to gate. Such feedback capacitors may impact the overall RF performance of the device especially at high frequencies. Systematic investigations on the small signal as well as power performance as functions of the drain biases are presented.

Keywords: field plate; AlGaN/GaN; HEMT; feedback; capacitors.

1. Introduction

Modern wireless communication systems have put extremely stringent requirements on both power and linearity performance of power amplifiers for base stations operating at microwave frequencies. In a lot of phased-array radar systems, highly reliable power amplifiers with good linearity are critical to guarantee the overall system performance since such systems always operate under harsh environmental conditions. Silicon LDMOS power transistors have dominated such applications over the past years. However, with the approaching limits of operability for such devices, there will be a need for other semiconductor materials to fulfill the high-power and high-linearity requirements of the next generation wireless technology. Gallium nitride (GaN) has been acknowledged as prime candidate for high-power

* Corresponding author. Tel.: +886-3-463-8800; fax: +886-3-455-4624.
E-mail address: htbeckhsu@saturn.yzu.edu.tw.

1875-3892 © 2012 Published by Elsevier B.V. Selection and/or peer-review under responsibility of Garry Lee
doi:10.1016/j.phpro.2012.03.054

microwave applications due to their high breakdown field (3MV/cm), high electron saturation velocity (2.5×10^7cm^2/V-s), and high operating temperature. [1] The associated AlGaN/GaN HEMT structure further features relatively high electron mobility due to the existence of the two-dimensional electron gases (2 DEGs). Such superior electronic properties of the structure have generated record-high output power densities at X- and Ku-band. [2,3]

Recently, a field plate structure has been widely used in AlGaN/GaN HEMTs for power application. It was believed that the field plate cannot only enhance breakdown voltage but also suppress the surface state, which markedly affected the power performance of GaN HEMTs. [4,5] The effects of insulator thickness and geometry of the field plate on breakdown voltage and frequency response were discussed. [4,6,7] Meanwhile, the extension gate of the field plate increases the gate capacitance (C_{gd}) and results in degraded transconductance (G_m) and gain characteristics. While studies have been focused on the effect of field plates to increase the breakdown voltage, not much research effort has been devoted to the impact on the overall RF performance of the field-plated (FP) AlGaN/GaN HEMT. [7,8] From the circuit point of view, the field plate behaves as a drain-to-gate feedback capacitor which provides additional modulation on the signals at the input and output of the device. Under such circumstances, impact on the RF performance is expected especially at high frequencies due to the additional phase variations provided through the feedback path. Thus, this study focuses on the systematic comparisons of the RF performance between field-plated and non field-plated devices under different bias conditions.

2. Device Fabrication

The AlGaN/GaN HEMT epitaxy structure in this study was grown on sapphire by metal organic chemical vapor deposition. The structure included 3-μm-thick undoped GaN buffer and 30-nm-thick undoped $Al_{0.25}Ga_{0.75}N$ layers. The Hall mobility and sheet carrier concentration were 1300 cm^2 V^{-1} s^{-1} and 1×10^{13} cm^{-2}, respectively. Fig. 1 shows a schematic cross section of the field-plated AlGaN/GaN HEMT.

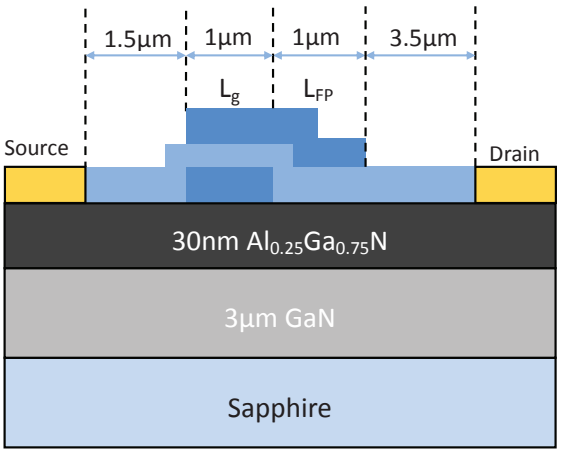

Fig. 1. The schematic cross section of the field-plated AlGaN/GaN HEMT device.

Mesa etching was performed by ICP-RIE with a Cl_2/BCl_3 gas mixture. Ohmic alloy Ti/Al/Ni/Au was deposited by e-beam evaporation and annealed in nitrogen atmosphere at 800 ℃ for 60 s. The spacing between source and drain was 7 μm. The ohmic contact resistance was 3×10^{-6} Ω cm^2. After ohmic

formation, the sample was dipped in dilute HCl for 1 min for cleaning. After cleaning, a Ni/Au gate (L_g = 1 μm) was deposited and subsequently the device was passivated with a 100-nm-thick SiN_x layer grown by plasma-enhanced chemical vapor deposition. Finally, Ti/Au was deposited as the field plate structure (L_{FP} = 1 μm), which was connected to the gate electrode. The device was 100 μm FET with gate finger widths of 50 μm. In this study, both FP and non-FP (nFP) AlGaN/GaN HEMTs were fabricated to observe the effect of the field plate structure on the RF characteristics at microwave frequencies.

3. Results and Discussions

3.1. DC Characteristics

Fig. 2 shows the DC I-V curves of the FP and nFP HEMT devices. Fig. 3 compares the G_m and drain current as a function of gate biases for both types of devices. As observed, the maximum drain current at V_{GS} = 0 was 610 mA/mm and the maximum transconductance was 160 mS/mm for the nFP HEMT, compared to those of 545mA/mm and 140mS/mm for the FP HEMT, respectively.

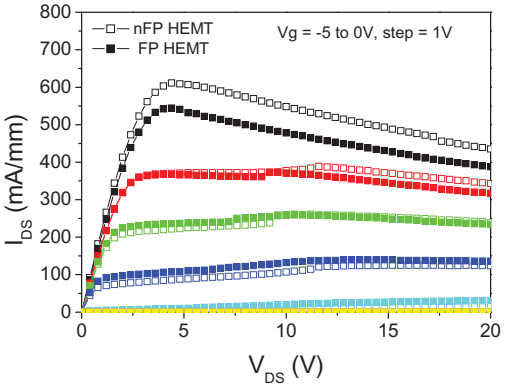

Fig. 2. DC I-V curves of FP-HEMT and nFP-HEMT

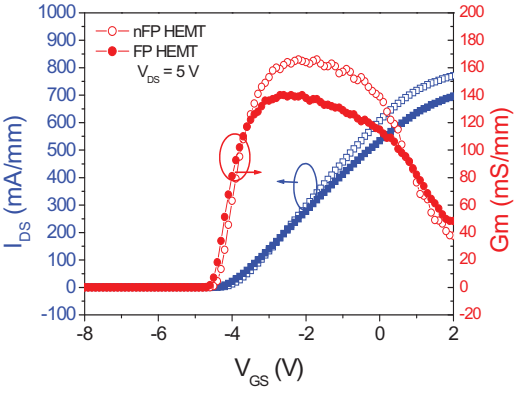

Fig. 3. The Gm and drain currents as functions of gate biases

Clearly, a 11% reduction of saturation drain current in the FP-HEMT is observed which is mainly due to the gate extension from the field plate structure. Such extension together with the thin SiNx passivation layer yields to a larger effective gate length causing degradation in the drain saturation current. Despite the degradation in saturation current, the FP-HEMT exhibited an improved breakdown voltage of 160 V compared with 90 V for the nFP-HEMT. The improvement in breakdown voltage makes higher drain bias possible leading to better power and linearity performance with good reliability.

3.2. Small Signal RF Performance

S-parameters of the 100 μm FP and nFP-HEMT devices were measured from 1 to 40 GHz using a Cascade Microtech on-wafer probing system with an HP8510XF vector network analyzer. Additionally, a standard load-reflection-reflection-match (LRRM) calibration method was used to calibrate the measurement system, and the calibrated reference planes were at the tips of the corresponding probes. The parasitic effects (mainly capacitive) from the probing pads have been carefully removed from the measured S-parameters using the same method as Yamashita *et al.* and the equivalent circuit model

reported by Dambrine *et al*. [9,10] Fig. 4 shows the extracted RF G_m and drain-to-gate capacitance (C_{gd}) as functions of the drain bias for the FP and nFP devices. Fig. 5 correspondingly shows the extracted gate-to-source capacitance (C_{gs}) as a function of the drain bias. The dependence of the cutoff frequency (f_T) on the drain biases for the FP and nFP devices is included in Fig. 6. In order to have a fair comparison, the gate biases for generating the three figures were chosen at the peak DC transconductance to accommodate for the slight shift in the threshold voltage for device with field plate.

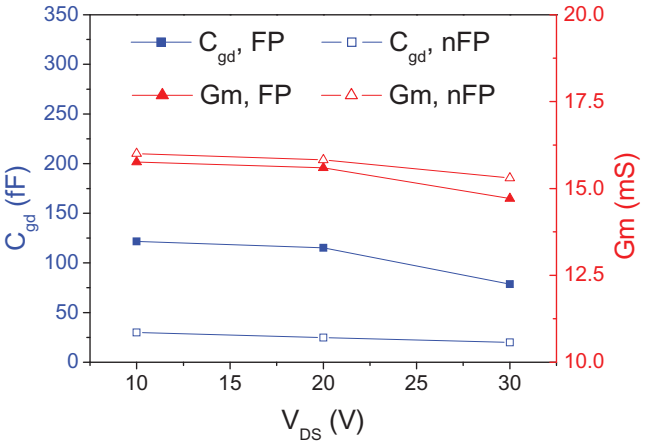

Fig. 4 Dependence of equivalent model parameters on drain bias for FP and nFP devices

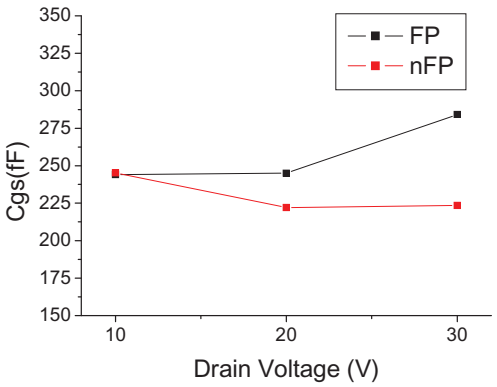

Fig. 5. Dependence of C_{gs} on drain bias for FP and nFP devices

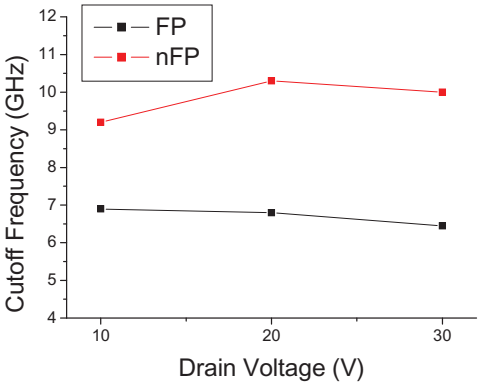

Fig. 6. Dependence of f_T on drain bias for FP and nFP devices

As expected, the extracted C_{gd} of FP device exhibited a major increase compared with that of nFP one. Moreover, the gate-to-source capacitance showed a minor increase with increasing drain bias. Fig. 6 shows the dependence of f_T on the drain bias for FP and nFP devices. Clearly, the FP devices showed a lower f_T due to the major increase in C_{gd} compared to the nFP devices. However, it is also relevant that the dependence of f_T on drain bias is very weak for FP devices.

3.3. RF Power Performance

The power performance was characterized using a FOCUS on-wafer load-pull system. The devices were tuned for the maximum output power. Fig. 7 shows the output power, gain, and PAE as a function of input power for both devices at 2 GHz when biased at 30 V with a 15 mA/mm current density. The optimum load reflection coefficients were $\Gamma_{opt} = 0.886\angle 9.9^{o}$ and $\Gamma_{opt} = 0.885\angle 7.5^{o}$ for FP and nFP devices, respectively. A higher output power of 25.36 dBm and PAE of 43% were achieved for the FP device. Meanwhile, P_{1dB} for the FP and nFP devices when biased at a 30V drain bias were 18.52 and 16.26 dBm, respectively. The softer gain compression of the FP device is believed to be the reason for the linearity improvement at high output power levels even beyond P_{1dB}. Such superior performance is mainly attributed to the reduction of trapping in surface states due to the field plate structure.

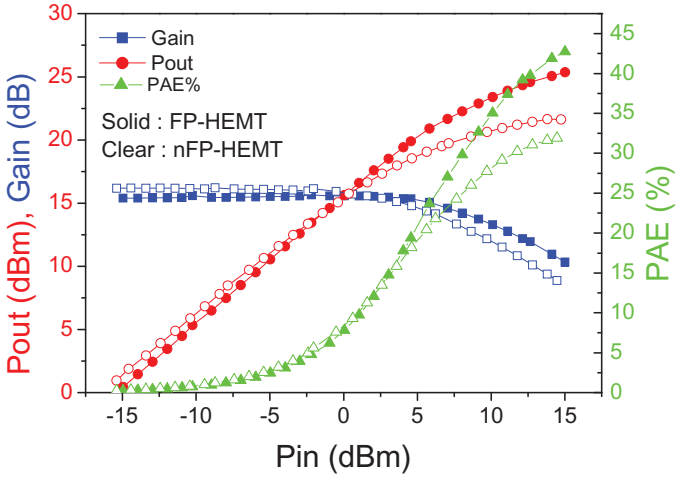

Fig. 7. The measured RF power performance at 2GHz when both devices were biased at 30V.

4. Conclusion

In this study, a field-plated AlGaN/GaN HEMT device has been fabricated and characterized. Measurement results revealed an output power of 25.36 dBm with a linear gain of 15.39 dB achieved for the FP-HEMT at 2 GHz when biased at V_{ds} = 30 V. An improvement in breakdown voltage from 90 to 160 V was observed. The major impact of the field plate on the device performance was the degradation in the cutoff frequency mainly due to the increase in the gate-to-drain capacitance. The softer gain compression of the FP devices was mainly attributed to the phase compensation provided through the feedback capacitance. Such observation has highlighted possible optimization on the field plate geometries for specific applications at the desired frequencies.

Acknowledgements

The authors would like to acknowledge the support from the National Science Council and the Ministry of Economic Affairs, Taiwan, R.O.C., under the contracts: NSC 99-2221-E-155-090 and NSC 100-2221-E-155-003.

References

[1] W. Nagy, J. Brown, R. Borges, and S. Singhal, “Linearity characteristics of microwave-power GaN HEMTs,” Microwave Theory Tech. Vol.51, 660-664 (2003).

[2] Y. Ando, Y. Okamoto, H. Miyamoto, T. Nakayama, T. Inoue, and M. Kuzuhara, “10-W/mm AlGaN-GaN HFET with a field modulating plate,” IEEE Electron Device Lett. Vol.24, 289-291 (2003).

[3] Y. Pei, R. Chu, L. Shen, N. Fichtenbaum, D. Brown, Z. Chen, S. Keller, S. P. DenBaars, and U. K. Mishra, “Effect of Al Composition and Gate Recess on Power Performance of AlGaN/GaN High-Electron Mobility Transistors,” IEEE Electron Device Lett. Vol.29, 300-302 (2008).

[4] Y.-F. Wu, A. Saxler, M. Moore, R. P. Smith, S. Sheppard, P. M. Chavarkar, T. Wisleder, U. K. Mishra, and P. Parikh, “30-W/mm GaN HEMTs by field plate optimization ,” IEEE Electron Device Lett. Vol.25, 117-119 (2004).

[5] Y. Okamoto, Y. Ando, K. Hataya, T. Nakayama, H. Miyamoto, T. Inoue, M. Senda, K. Hirata, M. Kosaki, N. Shibata, and M. Kuzuhara, “Improved power performance for a recessed-gate AlGaN-GaN heterojunction FET with a field-modulating plate,” IEEE Trans. microwave theory tech. Vol.52, 2536-2540 (2004).

[6] S. Karmalkar and U. K. Mishra, “Enhancement of breakdown voltage in AlGaN/GaN high electron mobility transistors using a field plate,” IEEE Trans. Electron Devices Vol.48, 1515-1521 (2001).

[7] H. Xing, Y. Dora, A. Chini, S. Heikman, S. Keller, and U. K. Mishra, “High breakdown voltage AlGaN-GaN HEMTs achieved by multiple field plates,” IEEE Electron Device Lett. Vol.25, 161-163 (2004).

[8] Y. Dora, A. Chakraborty, L. McCarthy, S. Keller, S. DenBarrs, and U. K. Mishra, “High Breakdown Voltage Achieved on AlGaN/GaN HEMTs With Integrated Slant Field Plates ,” IEEE Electron Device Lett. Vol.27, 713-715 (2006).

[9] Y. Yamashita, A. Endoh, K. Shinohara, M. Higashiwaki, K. Hikosaka, T. Mimura, S. Hiyamizu, and T. Matsui, “Ultra-short 25-nm-gate lattice-matched InAlAs/InGaAs HEMTs within the range of 400 GHz cutoff frequency,” IEEE Electron Device Lett. Vol.22, 367-369 (2001).

[10] G. Dambrine, A. Cappy, F. Heliodore, and E. Playez, “A new method for determining the FET small-signal equivalent circuit,” IEEE Trans. Microwave Theory Tech. Vol.36, 1151-1159 (1988).